

Oriented graph structure of local energy minima in the random-field Ising model

Paolo Bortolotti^{a,b,*}, Vittorio Basso^b, Alessandro Magni^b, Giorgio Bertotti^b

^aPolitecnico di Torino, Corso Duca degli Abruzzi 24, 10129 Torino, Italy

^bIstituto Nazionale di Ricerca Metrologica, Strada delle Cacce 91, 10135 Torino, Italy

Abstract

In this paper we investigate the structure of the disordered energy landscape of the RFIM with field-driven single-spin-flip dynamics. We show that local energy minima are partitioned into equivalence classes (basins) organized in a binary oriented graph. We discuss two algorithms by which one can explore the oriented graph structure.

© 2007 Elsevier B.V. All rights reserved.

PACS: 75.10.Nr; 75.60.Ej

Keywords: Random-field Ising model; Hysteresis modeling; Oriented graph

1. Introduction

Ferromagnetic materials exhibit hysteresis when they are driven by an external magnetic field h . The h field takes the system far from equilibrium, along a sequence of local energy minima resulting from the balance of exchange interactions, anisotropy, coupling with structural disorder and with the external field. The system moves from one local minimum to the next through discontinuous jumps (Barkhausen noise) where some energy is irreversibly transferred to the outer environment.

The random-field Ising model (RFIM) with single-spin-flip dynamics [1–4] is an interesting model system for the study of these phenomena. The system is represented by N Ising spins $s_i = \pm 1$ at each site of a D -dimensional lattice with periodic boundary conditions. Structural disorder is described by local independent random fields f_i , extracted from some distribution. We will consider the case when the distribution is Gaussian with zero mean value and variance σ^2 . The RFIM

Hamiltonian is thus:

$$\mathcal{H}(\{s_i\}, h) = -\frac{J}{2} \sum_{i=1}^N \sum_{j \in \mathcal{R}_i} s_i s_j - \sum_{i=1}^N (f_i + h) s_i, \quad (1)$$

where $J > 0$ and \mathcal{R}_i is the set of spins exchange-coupled to s_i .

A spin configuration $\omega = \{s_i\}$ at a given field h is said to be stable if flipping any individual spin leads to an increase of the system energy. Stable configurations satisfy the stability relation:

$$s_i = \text{sign}(h_i) \quad (2)$$

for all spin s_i , where h_i is the internal field acting on s_i :

$$h_i = J \sum_{j \in \mathcal{R}_i} s_j + f_i + h. \quad (3)$$

The single-spin-flip dynamics considered by most authors is based on the idea of continuously monitoring the stability condition (2) as the external field is varied in time. As soon as Eq. (2) is violated for some spin s_k (i.e., $s_k = +1$ and $h_k = 0^-$ or vice versa), spin s_k is flipped and spins made unstable by previous flips are reversed in sequence (Barkhausen avalanche) until a new stable configuration is reached. This dynamics is *rate-independent* because when

*Corresponding author. Politecnico di Torino, Corso Duca degli Abruzzi 24, 10129 Torino, Italy. Tel.: +39 011 3919841.

E-mail address: bortolo@inrim.it (P. Bortolotti).

the avalanche starts, the external field is not changed until a new stable configuration is reached.

An important notion in spin-flip dynamics is that of state ordering. Given a spin configuration ω at the field h , one defines the spin state \mathbf{s} as the pair $\mathbf{s} = (\omega, h)$. Two spins states $\mathbf{s} = (\omega, h)$ and $\mathbf{s}' = (\omega', h')$, with $\omega = \{s_i\}$ and $\omega' = \{s'_i\}$, are said to be ordered, i.e., $\mathbf{s} \leq \mathbf{s}'$, if $h \leq h'$ and $s_i \leq s'_i$ for every i . One can prove that RFIM single spin-flip dynamics is order-preserving and that, as a consequence of this property, RFIM exhibits return-point memory [1].

2. Hierarchical state organization

Given a generic stable state \mathbf{s} , a question of general interest is whether there exists a field history that generates an appropriate sequence of spin-flips bringing the system from one of the saturation states, i.e., $t_\infty^+ = (\{s_i = +1\}, h \rightarrow +\infty)$ or $t_\infty^- = (\{s_i = -1\}, h \rightarrow -\infty)$, to \mathbf{s} . A state which can be reached from saturation in this way is termed a field-reachable state or simply an h -state. Field-reachable states play an important role, because they are the ones involved in any study of field-driven magnetization curves. On the other hand, one would like to understand to what extent states generated by other types of external action, for example, through quenching from high temperatures, may also be generated by a suitable field history.

To answer this question, a constructive algorithm was developed in Ref. [5]. By taking advantage of the ordering properties of spin-flip dynamics, the algorithm is able to recognize whether a given stable state \mathbf{s} is field-reachable or not. When \mathbf{s} is field-reachable, the algorithm returns the list of field inversion points, i.e., the field history generating \mathbf{s} from saturation. Conversely, when \mathbf{s} is not field-reachable, the algorithm returns a field history terminating in the periodic generation of a pair of distinct states $(\mathbf{a}^-, \mathbf{a}^+)$ with the property that $\mathbf{a}^- \leq \mathbf{s} \leq \mathbf{a}^+$.

This algorithm says nothing about the organization of non-reachable states. In fact, a non-trivial and rich structure is revealed when one introduces the notion of *mutually connected* states: two stable states \mathbf{s} and \mathbf{s}' are said to be mutually connected if there exist two field histories transforming $\mathbf{s} \rightarrow \mathbf{s}'$ and $\mathbf{s}' \rightarrow \mathbf{s}$, respectively. Mutual connection is an equivalence relation which subdivides stable states into equivalence classes termed *basins* and denoted by B_l . The set of h -states is itself a basin denoted by B_∞ , namely the basin of mutually connected states also reachable from saturation [6,7]. It has been shown in Ref. [7] that a basin is fully identified by a pair $(\mathbf{t}^-, \mathbf{t}^+)$ of ordered states, $\mathbf{t}^- \leq \mathbf{t}^+$, termed *twin states*. Let (h^-, h^+) be the fields associated with $(\mathbf{t}^-, \mathbf{t}^+)$. Then, as long as one applies any field history within the interval (h^-, h^+) to a state belonging to the basin, one always obtains another state of the basin. Instead, whenever the field exceeds one of the two limit values h^\pm , one gets out of the basin passing through \mathbf{t}^+ under increasing field or \mathbf{t}^- under decreasing field. Once a state out of the basin is reached, no field

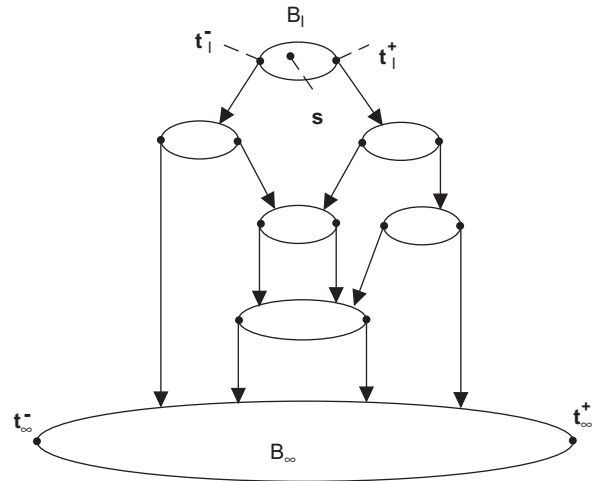


Fig. 1. Schematic representation of the oriented graph describing the basin structure of RFIM stable states. State \mathbf{s} is a generic state belonging to basin B_l . $(\mathbf{t}_l^-, \mathbf{t}_l^+)$ are twin states for B_l basin. $(\mathbf{t}_\infty^-, \mathbf{t}_\infty^+)$ are the saturation states, twin states of the basin of h -states B_∞ .

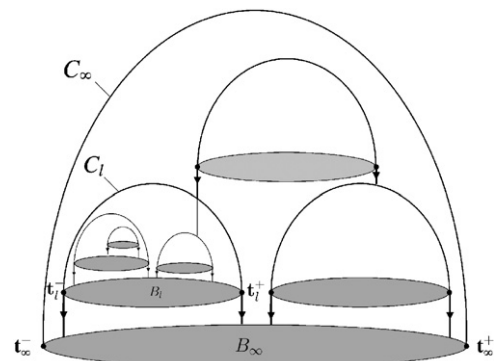


Fig. 2. Schematic representation of nested container structure.

history can bring the system back into the initial basin anymore.

As a result of these properties, basins turn out to be organized in a direct binary oriented graph, at the bottom of which there lies the basin B_∞ of field-reachable states (see Fig. 1).

A pair of twin states $(\mathbf{t}_l^-, \mathbf{t}_l^+)$ identifies also a *container* C_l [7], defined as the set of all states \mathbf{s} such that $\mathbf{t}_l^- \leq \mathbf{s} \leq \mathbf{t}_l^+$. The name container reflects the fact that a container will contain (in the sense of ordering) a certain number of basins, which will be themselves organized in containers and so on in a hierarchical nested fashion, as shown in Fig. 2. The container C_∞ identified by the saturation states $(\mathbf{t}_\infty^-, \mathbf{t}_\infty^+)$ contains all stable states, because $\mathbf{t}_\infty^- \leq \mathbf{s} \leq \mathbf{t}_\infty^+$ is satisfied for any \mathbf{s} (Fig. 2).

3. Algorithms for basin structure reconstruction

The algorithm presented in Ref. [5] tests if a state can be reached starting from one of the saturation states \mathbf{t}_∞^\pm . In this sense, it identifies field-reachable states for the container C_∞ . This algorithm can be generalized in a

natural way to states belonging to the generic container C_l defined by the twin states $(\mathbf{t}_l^-, \mathbf{t}_l^+)$. In this case, the algorithm will separate states belonging to the basin B_l defined by $(\mathbf{t}_l^-, \mathbf{t}_l^+)$, from states belonging not to B_l , but to one of the upper basins of the hierarchical structure inside C_l .

We define *characteristic curve* of a generic state \mathbf{s} the sequence of stable states obtained by monotonically increasing (ascending branch) or decreasing (descending branch) the external field starting from \mathbf{s} until one reaches the saturation states. If \mathbf{s} belongs to the container C_l , \mathbf{s} characteristic curve will pass through the twin states $(\mathbf{t}_l^-, \mathbf{t}_l^+)$ associated with C_l .

Then, given the state \mathbf{s} belonging to C_l , the generalization of the algorithm in Ref. [5] is defined by the following steps.

- (i) Construct \mathbf{s} characteristic curve.
- (ii) Start from \mathbf{t}_l^+ (\mathbf{t}_l^-).
- (iii) Decrease (increase) monotonically the field until one reaches a configuration belonging to \mathbf{s} characteristic curve.
- (iv) Invert the field variation and iterate step (iii).

By the same reasoning followed in Ref. [5] one proves that the algorithm can terminate in only one of the two following ways:

- (a) state \mathbf{s} is reached, which implies that \mathbf{s} belongs to B_l ;
- (b) the algorithm ends up in a loop between two states \mathbf{a}^\pm such that $\mathbf{a}^- \leq \mathbf{s} \leq \mathbf{a}^+$, in which case \mathbf{s} belongs to C_l but not to B_l .

The field history generated by the algorithm is termed *characteristic history* for state \mathbf{s} . The algorithm itself will be termed *characteristic algorithm*.

On this basis, we now construct an algorithm which, starting from a state \mathbf{s} of the container C_l with twin states $(\mathbf{t}_l^-, \mathbf{t}_l^+)$, identifies a new container C_m inside C_l , i.e., with twin states $(\mathbf{t}_m^-, \mathbf{t}_m^+)$ such that: $\mathbf{t}_l^- \leq \mathbf{t}_m^- \leq \mathbf{t}_m^+ \leq \mathbf{t}_l^+$. Such procedure will be termed *upward algorithm* due to the fact that it permits one to go one step *upstream* in the nested container structure. This algorithm can be applied every time the characteristic algorithm returns a pair of distinct states \mathbf{a}^\pm . The upward algorithm is defined by the following steps.

- (i) Apply the characteristic algorithm to a state \mathbf{s} belonging to C_l but not reachable from \mathbf{t}_l^\pm , i.e., not belonging to B_l . The algorithm returns the states \mathbf{a}^\pm .
- (ii) Take the state \mathbf{a}^+ (a similar argument applies to \mathbf{a}^-). Decrease the field and list the stable spin configurations ω_k generated by the spin-flip dynamics when going from \mathbf{a}^+ to \mathbf{a}^- .
- (iii) For each configuration ω_k , construct the corresponding increasing-field return branch and let ω_k^+ be the

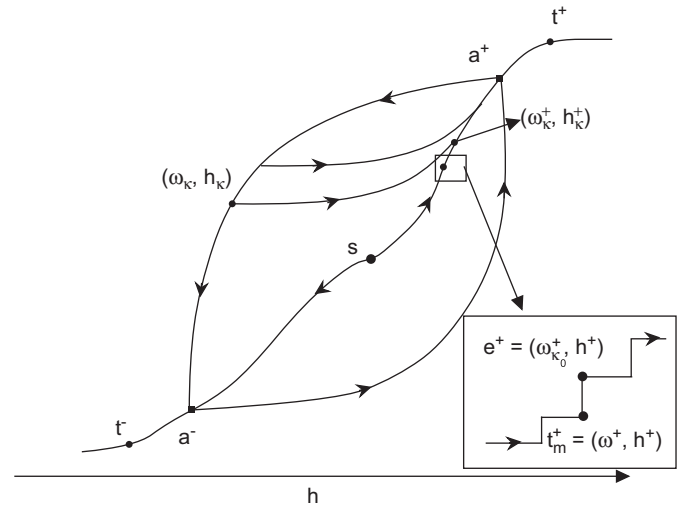


Fig. 3. Schematic representation of states involved in upward algorithm.

spin configuration at which the return branch hits \mathbf{s} characteristic curve (see Fig. 3).

- (iv) Since the configurations ω_k^+ all belong to \mathbf{s} characteristic curve, they are all ordered. Let $\omega_{k_0}^+$ be the minimum one, i.e., $\omega_{k_0}^+ \leq \omega_k^+$ for every k .
- (v) Traverse \mathbf{s} characteristic curve starting from \mathbf{s} under increasing field and look for the state $\mathbf{t}_m^+ = (\omega^+, h^+)$ where the system jumps from \mathbf{t}_m^+ to $\mathbf{e}^+ = (\omega_{k_0}^+, h^+)$. Then \mathbf{t}_m^+ is the upper twin state of a container C_m inside C_l , and \mathbf{e}^+ is the point of entrance of \mathbf{s} characteristic curve into basin B_l .

Once \mathbf{t}_m^+ is known, its companion state \mathbf{t}_m^- can be found by generating the lower branch of \mathbf{t}_m^+ characteristic curve and checking the mutual connection of states on this branch with \mathbf{t}_m^+ itself.

The proof that the state \mathbf{t}_m^+ identified by the upward algorithm is indeed a twin state is given in Appendix A.

By the upward algorithm, given a container C_l and a state \mathbf{s} belonging to C_l , one identifies a new container C_m contained in C_l . In general, \mathbf{s} will not be contained in C_m , i.e., the inequality $\mathbf{t}_m^- \leq \mathbf{s} \leq \mathbf{t}_m^+$ will not be fulfilled. However, one can consider at this point a new state $\mathbf{s}' \neq \mathbf{s}$ inside C_m , i.e., $\mathbf{t}_m^- \leq \mathbf{s}' \leq \mathbf{t}_m^+$, and apply again the upward algorithm in order to identify a new container C_p inside C_m . This procedure can be iterated in order to generate a sequence of nested containers. The iteration will terminate when two twin states $(\mathbf{t}_f^-, \mathbf{t}_f^+)$ are found such that the container C_f identified by them contains a single basin, i.e., $C_f \equiv B_f$. These top-level elementary containers are expected to play a special role in the model.

The sequence of nested containers C_l, C_m, C_p, \dots has an interesting physical interpretation. In fact, the container C_l corresponds to a partition of spins $\{s_i\}$ into two classes, that is: the *active* spins which are equal to -1 in state \mathbf{t}_l^- and to $+1$ in state \mathbf{t}_l^+ ; the *inactive* spins whose orientation is the same in \mathbf{t}_l^- and \mathbf{t}_l^+ . Any state \mathbf{s} belonging to the container, i.e., $\mathbf{t}_l^- \leq \mathbf{s} \leq \mathbf{t}_l^+$, is a state for which the active

spins are partly equal to +1 and partly to -1. The existence of a container C_m inside C_l corresponds to the fact that part of C_l active spins become inactive when states inside C_m are considered. Therefore, the sequence of nested containers previously discussed is associated with a sequence of progressively fewer active spins, and the top level container of the sequence will correspond to minimal groups of spins which can be flipped back and forth in an appropriate field interval without affecting the remaining spins. The physical consequences of this interpretation will be investigated in future work.

Appendix A

To prove that the state \mathbf{t}_m^+ in Fig. 3 is a twin state it is enough to prove that it does not belong to basin B_l associated with $(\mathbf{t}_l^-, \mathbf{t}_l^+)$. In fact, since \mathbf{s} characteristic curve goes from \mathbf{t}_m^+ to \mathbf{e}^+ in one jump and \mathbf{e}^+ does belong to B_l , then \mathbf{t}_m^+ will be the point of exit from some other basin, i.e., a twin state. Here we give a sketch of the proof. We denote by $\mathbf{b}_+(\mathbf{s})$ and $\mathbf{b}_-(\mathbf{s})$ the ascending and descending branches of the characteristic curve of a given state \mathbf{s} , respectively. Let us consider $\mathbf{b}_-(\mathbf{e}^+)$ and let \mathbf{e}_1 be the point where this branch touches $\mathbf{b}_-(\mathbf{a}^+)$. Similarly, let \mathbf{t}_1 be the point when $\mathbf{b}_-(\mathbf{t}_m^+)$ touches $\mathbf{b}_-(\mathbf{a}^+)$. By construction

$\mathbf{a}^- \leq \mathbf{t}_1 \leq \mathbf{e}_1$. In order to determine whether \mathbf{t}_m^+ belongs to basin B_l or not, we apply the characteristic algorithm to \mathbf{t}_m^+ . If $\mathbf{t}_1 \equiv \mathbf{a}^-$, the characteristic algorithm will return the state pair $(\mathbf{a}^-, \mathbf{a}^+)$, which means that \mathbf{t}_m^+ does not belong to B_l . Let us then consider the case when $\mathbf{t}_1 \neq \mathbf{a}^-$. Let \mathbf{t}_2 be the point where $\mathbf{b}_+(\mathbf{t}_1)$ first touches $\mathbf{b}_+(\mathbf{t}_m^+)$. The case $\mathbf{t}_2 \leq \mathbf{t}_m^+$ is not possible, because this would contradict the definition of \mathbf{e}^+ . Therefore $\mathbf{t}_2 \geq \mathbf{e}^+$. This implies that applying the characteristic algorithm to \mathbf{t}_m^+ will return the state pair $(\mathbf{t}_1, \mathbf{t}_2)$, which means that also in this case \mathbf{t}_m^+ does not belong to B_l .

References

- [1] J.P. Sethna, et al., Phys. Rev. Lett. 70 (1993) 21; J.P. Sethna, et al., in: G. Bertotti, I.D. Mayergoyz (Eds.), The Science of Hysteresis, vol. II, Academic Press, New York, 2006.
- [2] E. Vives, A. Planes, J. Magn. Magn. Mater. 164–171 (2000) 221.
- [3] L. Dante, G. Durin, A. Magni, S. Zapperi, Phys. Rev. B 65 (2002) 144441.
- [4] M.J. Alava, V. Basso, F. Colaiori, L. Dante, G. Durin, A. Magni, S. Zapperi, Phys. Rev. B 71 (2005) 064423.
- [5] V. Basso, A. Magni, Physica B 343 (2004) 275.
- [6] A. Magni, V. Basso, J. Magn. Magn. Mater. 290–291 (2005) 460.
- [7] G. Bertotti, P. Bortolotti, A. Magni, V. Basso, J. Appl. Phys. 101 (2007) 09D508.